

light was required to afford water decomposition. With respect to  $\text{Cr}^{3+}$ -doped  $\text{TiO}_2$  electrodes, the colloidal semiconductor particles have the advantage that the small minority carrier diffusion length does not decrease the quantum yield of  $\text{H}_2$  formation from band-gap excitation. The use of very small semiconductor particles was combined here with the concept of electrocatalysis for water reduction and oxidation by ultrafine noble metal deposits. A striking synergistic effect was shown to be operative between  $\text{RuO}_2$  and Pt, underlining again the superiority of this catalyst combination in water photolysis systems.

(40) (a) Bulatov, A. V.; Khidekel, M. L. *Izv. Akad. Nauk SSSR, Ser. Khim.* 1976, 1902. (b) Schrauzer, G. N.; Guth, T. D. *J. Am. Chem. Soc.* 1977, 99, 7189. (c) van Damme, H.; Hall, W. K. *Ibid.* 1979, 101, 4373. (d) Sato, S.; White, J. M. *Chem. Phys. Lett.* 1980, 72, 83. (e) Kawai, T.; Sakata, T. *Ibid.* 1980, 72, 87. (f) Domen, K.; Naito, S.; Sorna, M.; Onishi, T.; Tamura, K. *J. Chem. Soc., Chem. Commun.* 1980, 543. (g) Kawai, T.; Sakata, T. *Nature (London)* 1980, 286, 474. (h) Wagner, F. T.; Somorjai, G. A. *Ibid.* 1980, 285, 559. (i) Lehn, J. M.; Sauvage, J. P.; Ziessel, R. *Nouv. J. Chim.* 1980, 4, 623. (j) Sato, S.; White, J. M. *J. Catal.* 1981, 69, 128.

Important information has also been obtained on the role of the  $\text{TiO}_2$  support material as an oxygen carrier. Photouptake of  $\text{O}_2$  by our hydroxylated anatase decreases the concentration of free oxygen in solution, which allows light-induced water cleavage to proceed at a high yield. The buildup of  $\text{O}_2$  is a key problem in all devices that attempt to cogenerate  $\text{H}_2$  and  $\text{O}_2$  without local separation, since the latter competes with protons for reduction on Pt sites. Further studies will therefore be directed to increase the capacity for  $\text{O}_2$  uptake of the system. Through introduction of supplementary heterogeneous oxygen carriers, it should be possible to develop systems that under solar irradiation will produce pure hydrogen, oxygen being retained on a carrier that releases it during the night.

**Acknowledgment.** This work was supported by the Swiss National Science Foundation and in part by CIBA Geigy, Basel. E.P. thanks the CNR, Italy, for support.

**Registry No.**  $\text{TiO}_2$ , 13463-67-7;  $\text{RuO}_2$ , 12036-10-1;  $\text{Cr}^{3+}$ , 16065-83-1; Pt, 7440-06-4;  $\text{H}_2\text{O}$ , 7732-18-5.

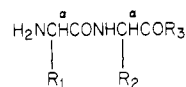
## Ground- and Excited-State Conformational Differences between Diastereomeric Dipeptides

Chieu D. Tran, Godfrey S. Beddard, Rose McConnell, Charles F. Hoyng, and Janos H. Fendler\*

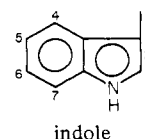
Contribution from the Department of Chemistry, Texas A&M University, College Station, Texas 77843. Received October 20, 1980

**Abstract:** Ground- and excited-state conformations of D-tryptophanyl-L-tryptophan methyl ester ( $1_{\text{DL}}$ ) L-tryptophanyl-L-tryptophan methyl ester ( $1_{\text{LL}}$ ) have been investigated by  $^1\text{H}$  NMR and by steady-state and subnanosecond time-resolved fluorescence lifetime and anisotropy measurements. Examination of  $^1\text{H}$  NMR spectra of cyclic L-tryptophanyl-L-tryptophan and of  $1_{\text{DL}}$  and  $1_{\text{LL}}$  at different temperatures suggested that the two indole rings are close to each other in  $1_{\text{DL}}$  but not in  $1_{\text{LL}}$ . Fluorescence decays of  $1_{\text{DL}}$  and  $1_{\text{LL}}$  in  $\text{Me}_2\text{SO}$  and  $\text{MeOH}$  and in glycerol-methanol mixtures have been fitted to  $I(t) = A[e^{-t/\tau_1} + (1-f)e^{-t/\tau_2}] + B$ , where  $\tau_1$  and  $\tau_2$  are fluorescence decay times,  $A$  is the amplitude, and  $B$  is the background. Differences in the mean decay times,  $\tau_m$  ( $\tau_m = f\tau_1 + (1-f)\tau_2$ ), between  $1_{\text{DL}}$  and  $1_{\text{LL}}$  reflected different degrees of quenching of the chromophores due to different conformations. No diastereomeric selectivity has been observed, however, in the quenching of  $\tau_m$  by  $\text{CCl}_4$ . Plots of rotational correlation times,  $\tau_R$  values, against solvent viscosities for  $1_{\text{DL}}$  and  $1_{\text{LL}}$  gave slopes of 21.2 and 17.1 ps/cP, respectively. These values are larger than those expected from the Stokes-Einstein equation, assuming the stick boundary conditions. The observed  $\tau_R$  values for  $1$  have been discussed in terms of four possible behaviors related to rapid or fixed motions of the two tryptophans and to the fast and slow energy transfers between the two indole moieties during the excited-state lifetime as well as in terms of long-lived volume fluctuations of the solvent.

Differences in chemical and physical properties of diastereomers have been the subject of much theoretical<sup>1,2</sup> and experimental<sup>3-5</sup> studies. Diastereomeric differences in dipeptides are particularly important since protein folding is affected by side-chain conformations.<sup>6,7</sup> Ground- and excited-state conformations of D-tryptophanyl-L-tryptophan methyl ester ( $1_{\text{DL}}$ ) and L-tryptophanyl-L-tryptophan methyl ester ( $1_{\text{LL}}$ ) have been investigated in the present work, therefore, by  $^1\text{H}$  NMR and by steady-state and subnanosecond time-resolved fluorescence anisotropy. Introducing an indole moiety into the dipeptides enhances the differences in chemical shifts between the diastereomers.<sup>8</sup> Methyl esters were chosen to alleviate problems associated with protein transfer.<sup>9</sup> Ground-state conformational differences between diastereomeric  $1$  have been investigated by  $^1\text{H}$  NMR spectroscopy. The importance of intrinsic fluorescence of tryptophan residues in proteins<sup>10-12</sup> has prompted us to place greater emphasis on subnanosecond time resolved fluorescence spectroscopy which provided information on excited-state conformations of these dipeptides.



- 1,  $\text{R}_1 = \text{C}^{\beta}\text{H}_2\text{-indole}$ ,  $\text{R}_2 = \text{C}^{\beta}\text{H}_2\text{-indole}$ ,  $\text{R}_3 = \text{OMe}$   
 $1_{\text{LL}}$ , L-Trp-L-Trp-OMe  
 $1_{\text{DL}}$ , D-Trp-L-Trp-OMe  
 $1_{\text{DD}}$ , D-Trp-D-Trp-OMe  
 $1_{\text{LD}}$ , L-Trp-D-Trp-OMe  
 2,  $\text{R}_1 = \text{CH}_2\text{-indole}$ ,  $\text{R}_2 = \text{CH}_3$ ,  $\text{R}_3 = \text{OH}$  (L-Trp-L-Ala-OH)  
 3,  $\text{R}_1 = \text{CH}_3$ ,  $\text{R}_2 = \text{CH}_2\text{-indole}$ ,  $\text{R}_3 = \text{OH}$  (L-Ala-L-Trp-OH)



indole

The obtained results have been rationalized in terms of a folded structure for  $1_{\text{DL}}$  in which the two indole rings are approximately

\* To whom correspondence should be addressed at Clarkson College of Technology, Potsdam, NY 13676.

(1) Craig, D. P.; Mellor, D. P. *Fortschr. Chem. Forsch.*, 1976, 63, 1.

perpendicular to each other and in terms of a more open arrangement for **1<sub>DL</sub>**.

### Experimental Section

The tryptophanyltryptophan dipeptide methyl esters used in this study were obtained in two reaction steps. Mixed carbonic anhydride coupling of *N*-(benzyloxycarbonyl)-L(or D)-tryptophan,<sup>13,14</sup> with L(or D)-tryptophan methyl ester (Sigma) in *N,N*-dimethylformamide, provided *N*-(benzyloxycarbonyl)-L(or D)-tryptophanyl-L(or D)-tryptophan methyl ester. Removal of the *N*-benzyloxycarbonyl-protecting group via catalytic hydrogenolysis obtained L(or D)-tryptophanyl-L(or D)-tryptophan methyl ester, isolated as the hydrochloride salt. All peptides and peptide derivatives were homogeneous by thin-layer chromatographic analysis, displayed satisfactory physical constants, and were characterized spectroscopically.

***N*-(Benzyloxycarbonyl)tryptophanyltryptophan Methyl Ester. General Procedure.** A solution of 3.38 g (10 mmol) of *N*-(Benzyloxycarbonyl)-L(or D)-tryptophan in 100 mL of anhydrous *N,N*-dimethylformamide was chilled to  $-10^{\circ}\text{C}$ , vigorously stirred, and treated with 1.38 mL (1.01 g, 10 mmol) of triethylamine. After a period of 5 min, 1.09 g (10 mmol) of ethyl chloroformate was added. The reaction mixture was stirred at  $-10^{\circ}\text{C}$  for 30 min and then treated with a pre-cooled solution of 2.55 g (10 mmol) of L(or D)-tryptophan methyl ester hydrochloride (Sigma) in 100 mL of anhydrous *N,N*-dimethylformamide containing 1.38 mL (1.01 g, 10 mmol) of triethylamine. The mixture was stirred at  $-10^{\circ}\text{C}$  for 3 h and then overnight at room temperature. The solution was partitioned between ethyl acetate and 1 *N* aqueous hydrochloric acid. The organic layer was washed with equal volume quantities of 1 *N* aqueous hydrochloric acid, 5% aqueous sodium bicarbonate, and distilled water, dried over anhydrous sodium sulfate, and then evaporated under reduced pressure to obtain a white solid. The solid was recrystallized from dichloromethane-petroleum ether to yield *N*-(benzyloxycarbonyl)-L(or D)-tryptophanyl-L(or D)-tryptophan methyl ester.

***N*-(Benzyloxycarbonyl)-D-tryptophanyl-L-tryptophan Methyl Ester:** 4.52 g (84%); mp  $194\text{--}197^{\circ}\text{C}$ ;  $R_f$  0.51 ( $S_1$ );  $[\alpha]_D^{25} -11.1^{\circ}$  (*c* 1.0, methanol),  $4.2^{\circ}$  (*c* 1.0, acetone);  $^1\text{H}$  NMR ( $\text{CD}_3\text{COCD}_3$ )  $\delta$  3.17 (d,  $J = 7$  Hz, 4 H), 3.55 (s, 3 H), 4.20–4.78 (m, 2 H), 4.98 (s, 2 H), 6.80–7.50 (m, 16 H).

***N*-(Benzyloxycarbonyl)-D-tryptophanyl-L-tryptophan Methyl Ester:** 4.79 g (89%); mp  $205\text{--}206^{\circ}\text{C}$ ;  $R_f$  0.50 ( $S_1$ );  $[\alpha]_D^{25} 6.1^{\circ}$  (*c* 1.0, methanol),  $23.1^{\circ}$  (*c* 1.0, acetone);  $^1\text{H}$  NMR ( $\text{CD}_3\text{COCD}_3$ )  $\delta$  3.18 (d,  $J = 7$  Hz, 4 H), 3.53 (s, 3 H), 4.15–4.82 (m, 2 H), 5.00 (s, 2 H), 6.76–7.62 (m, 16 H).

***N*-(Benzyloxycarbonyl)-D-tryptophanyl-D-tryptophan Methyl Ester:** 4.36 g (81%); mp  $196\text{--}198^{\circ}\text{C}$ ;  $R_f$  0.52 ( $S_1$ );  $[\alpha]_D^{25} 10.5^{\circ}$  (*c* 1.0, methanol),  $-3.8^{\circ}$  (*c* 1.0, acetone);  $^1\text{H}$  NMR ( $\text{CD}_3\text{COCD}_3$ )  $\delta$  3.18 (d,  $J = 7$  Hz, 4 H), 3.52 (s, 3 H), 4.31–4.87 (m, 2 H), 4.99 (s, 2 H), 6.80–7.70 (m, 16 H).

***N*-(Benzyloxycarbonyl)-L-tryptophanyl-D-tryptophan Methyl Ester:** 4.14 g (77%); mp  $199\text{--}201^{\circ}\text{C}$ ;  $R_f$  0.50 ( $S_1$ );  $[\alpha]_D^{25} -7.9^{\circ}$  (*c* 1.0, methanol),  $-22.2^{\circ}$  (*c* 1.0, acetone);  $^1\text{H}$  NMR ( $\text{CD}_3\text{COCD}_3$ )  $\delta$  3.15 (d,  $J = 7$  Hz), 3.57 (s, 3 H), 4.12–4.88 (m, 2 H), 5.00 (s, 2 H), 6.80–7.70 (m, 16 H).

**Tryptophanyltryptophan Methyl Ester Hydrochloride (1). General Procedure.** A solution of 500 mg (0.93 mmol) of *N*-(benzyloxycarbonyl)-L(or D)-tryptophanyl-L(or D)-tryptophan methyl ester in 500 mL of methanol and 1 mL of 1 *N* aqueous hydrochloric acid was purged with hydrogen gas and stirred under a hydrogen atmosphere. A slurry of 500 mg of 10% palladium on charcoal in methanol was added. The mixture was stirred under a hydrogen atmosphere for 3 h. The catalyst was removed by filtration through activated charcoal. The filtrate was evaporated under reduced pressure in the dark at room temperature and

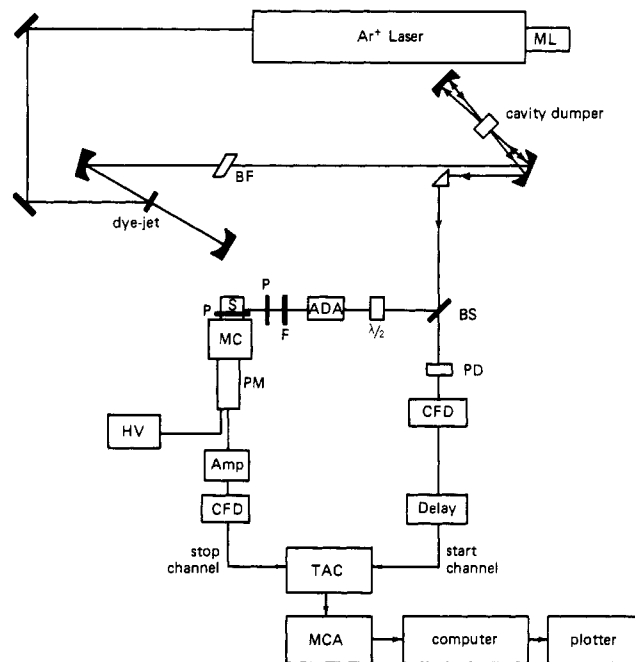


**Figure 1.** Block diagram of the synchronously pumped mode-locked cavity-dumped dye laser single-photon-counting instrument. Abbreviations: ML = model locker, BF = birefringe turning element in the jet stream dye laser, BS = beam splitter, F = filter, ADA = temperature tuned second harmonic generator, S = sample, P = polarizer, MC = monochromator, PM = photomultiplier, CFD = constant fraction discriminator, TAC = time to amplitude converter, HV = high voltage power supply, PD = photodiode, and MCA = multichannel analyzer.

then diluted with diethyl ether to induce crystallization. The solid product was collected, redissolved in methanol, filtered through activated charcoal, and recrystallized by dilution with diethyl ether. All operations were performed in the dark at room temperature.

**L-Tryptophanyl-L-tryptophan Methyl Ester Hydrochloride (**1<sub>LL</sub>**):** 391 mg (89%);  $R_f$  0.21 ( $S_2$ ), 0.76 ( $S_3$ );  $[\alpha]_D^{25} 14.6^{\circ}$  (*c* 1.0, *N,N*-dimethylformamide);  $^1\text{H}$  NMR ( $\text{CD}_3\text{CN}/\text{D}_2\text{O}$ )  $\delta$  3.20 (d,  $J = 7$  Hz, 4 H), 3.49 (s, 3 H), 7.00–7.65 (m, 11 H).

**D-Tryptophanyl-L-tryptophan Methyl Ester Hydrochloride (**1<sub>DL</sub>**):** 369 mg (84%);  $R_f$  0.15 ( $S_2$ ), 0.78 ( $S_3$ );  $[\alpha]_D^{25} -14.5^{\circ}$  (*c* 1.0, *N,N*-dimethylformamide);  $^1\text{H}$  NMR ( $\text{CD}_3\text{CN}$ )  $\delta$  3.15 (d,  $J = 7$  Hz, 4 H), 3.52 (s, 3 H), 4.15–4.90 (m, 2 H), 6.70–7.60 (m, 11 H).

**D-Tryptophanyl-D-tryptophan Methyl Ester Hydrochloride (**1<sub>DD</sub>**):** 396 mg (90%);  $R_f$  0.29 ( $S_2$ ), 0.73 ( $S_3$ );  $[\alpha]_D^{25} -16.5^{\circ}$  (*c* 1.0, *N,N*-dimethylformamide);  $^1\text{H}$  NMR ( $\text{CD}_3\text{CN}$ )  $\delta$  3.10 (d,  $J = 7$  Hz, 4 H), 3.55 (s, 3 H), 3.90–4.90 (m, 2 H), 6.75–7.80 (m, 11 H).

**L-Tryptophanyl-D-tryptophan Methyl Ester Hydrochloride (**1<sub>LD</sub>**):** 343 mg (78%);  $R_f$  0.26 ( $S_2$ ), 0.67 ( $S_3$ );  $[\alpha]_D^{25} 11.6^{\circ}$  (*c* 1.0, *N,N*-dimethylformamide);  $^1\text{H}$  NMR ( $\text{D}_2\text{O}$ )  $\delta$  3.20 (d,  $J = 7$  Hz, 4 H), 3.55 (s, 3 H), 6.75–7.80 (m, 11 H).

Glycerol (Baker's spectroscopic anhydrous grade) was twice vacuum distilled over activated charcoal. All other reagents were of spectroscopic grade.

All melting points were uncorrected.  $^1\text{H}$  were recorded on samples of 1.0 mg of dipeptide/0.5 mL of solvent using a Varian XL-200 MHz instrument. Chemical shifts are reported as  $\delta$  values in parts per million relative to tetramethylsilane ( $\delta_{\text{Me}_4\text{Si}} = 0.0$ ) as an internal standard. Optical rotations were determined on a Perkin-Elmer Model 241 polarimeter.

Fluorescence measurements were carried out on freshly prepared air-saturated solutions of  $5 \times 10^{-5}$  M **1** (DL or LL) at  $25.0 \pm 0.1^{\circ}\text{C}$ . Steady-state fluorescence spectra were measured on a SPEX Fluorolog spectrofluorimeter using the E/R mode. Generally, 2.5-mm slits were used. Steady-state polarizations were determined by placing a Gian-Thompson polarizer in the excitation beam and a Polaroid polarizer in the emission beam.<sup>15</sup>

The fluorescence lifetimes were measured by using the single-photon-counting apparatus shown in Figure 1 and briefly described below. The jet-stream dye laser (Spectra Physics 375 tunable dye laser) was synchronously pumped by the 514.5-nm line of an acousto-optically

- (2) Mason, S. F. *Ann. Rep. Chem. Soc.* **1976**, A73, 53.
- (3) Tran, C. D.; Fendler, J. H. *J. Am. Chem. Soc.* **1980**, 100, 2923.
- (4) Wynberg, H.; Feringa, B. *Tetrahedron* **1976**, 32, 2831.
- (5) Horeau, A.; Gvette, J. P. *Tetrahedron* **1974**, 30, 1923.
- (6) Lehninger, A. L. In "Biochemistry", 2nd ed.; Worth Publishers, Inc.: New York, 1975; Chapter 6.
- (7) Dickerson, R. F.; Geis, I. In "The Structure and Action of Proteins"; W.A. Benjamin: Menlo Park, Calif., 1969.
- (8) Wieland, Th.; Bende, H. *Chem. Ber.* **1965**, 98, 504.
- (9) Robbins, R. J.; Fleming, G. K.; Beddard, G. S.; Robinson, G. W.; Thistlethwaite, P. J. *J. Am. Chem. Soc.* **1980**, 102, 6271.
- (10) Grinvald, A.; Steinberg, I. Z. *Biochim. Biophys. Acta* **1976**, 427, 663.
- (11) Lakowicz, J. R.; Cherek, H. J. *Biol. Chem.* **1980**, 255, 831.
- (12) Munro, I.; Pecht, I.; Stryer, L. *Proc. Natl. Acad. Sci. U.S.A.* **1979**, 76, 56.
- (13) Smith, E. L. *J. Biol. Chem.* **1948**, 175, 39.
- (14) Yajima, H.; Kubo, K. *J. Am. Chem. Soc.* **1965**, 87, 2039.

- (15) Kano, K.; Fendler, J. H. *Chem. Phys. Lipids*, **1979**, 23, 189.

Table I.  $^1\text{H}$  NMR Chemical Shifts of Diastereomeric Dipeptides in  $\text{Me}_2\text{SO}-d_6$  at  $30^\circ\text{C}^a$ 

compd	$\text{R}_1$ -residue		$\text{R}_2$ -residue		$\text{R}_3$ -residue $\text{OCH}_3$	aromatic residue
	$\text{H}_\alpha$	$\text{H}_\beta$	$\text{H}_\alpha$	$\text{H}_\beta$		
2	4.14 (t)	3.00 (m)	3.63 (q)	1.26 (t)		7.20 (H-2, d), 7.61 (H-4, d), 7.28 (H-5(6), m), 7.36 (H-7, d)
3	3.48 (q)	1.20 (t)	4.42 (t)	3.18 (t)		7.12 (H-2, d), 7.54 (H-4, d), 7.00 (H-5(6), m), 7.32 (H-7, d)
1 <sub>LL</sub>	4.65 (m)	2.84 (m), 3.14 (m) <sup>b</sup>	4.06 (m)	2.84 (m), ~3.17 (m)	1.14 (s)	7.68 (H-4 of $\text{R}_1$ or $\text{R}_2$ , d), 7.48 (H-4 of $\text{R}_1$ or $\text{R}_2$ , d), 7.34 (H-7 of $\text{R}_1$ and $\text{R}_2$ , m), 7.19 (H-2 of $\text{R}_1$ and $\text{R}_2$ , s)
1 <sub>DD</sub>	4.06 (m)	2.84 (m), 3.14 (m) <sup>b</sup>	4.06 (m)	2.84 (m), ~3.17 (m)	1.14 (s)	6.68 (H-4 of $\text{R}_1$ or $\text{R}_2$ , d), 7.48 (H-4 of $\text{R}_1$ or $\text{R}_2$ , d), 7.34 (H-7 of $\text{R}_1$ and $\text{R}_2$ , m), 7.19 (H-2 of $\text{R}_1$ and $\text{R}_2$ , s)
1 <sub>DL</sub>	4.59 (m)	2.86 (m), ~3.16 (m) <sup>b</sup>	4.06 (m)	2.86 (m), 3.17 (m)	1.16 (s)	7.51 (H-4 of $\text{R}_1$ and $\text{R}_2$ , t), 7.32 (H-7 of $\text{R}_1$ and $\text{R}_2$ , m), 7.09 and 7.11 (H-2 of $\text{R}_1$ and $\text{R}_2$ , dd), 6.95 (H-5(6) of $\text{R}_1$ and $\text{R}_2$ , m)
1 <sub>LD</sub>	4.59 (t)	2.86 (m)	4.06 (q)	2.86 (m)	1.16 (s)	7.51 (H-4 of $\text{R}_1$ and $\text{R}_2$ , t), 7.32 (H-7 of $\text{R}_1$ and $\text{R}_2$ , m), 7.09 and 7.11 (H-2 of $\text{R}_1$ and $\text{R}_2$ , dd), 6.95 (H-5(6) of $\text{R}_1$ and $\text{R}_2$ , m)
cyclic L-Trp-L-Trp	4.14 ( $\text{H}_\alpha$ of $\text{R}_1$ and $\text{R}_2$ , t), 3.25 ( $\text{H}_\beta$ of $\text{R}_1$ and $\text{R}_2$ , m)					7.53 (H-4 of $\text{R}_1$ and $\text{R}_2$ , m), 7.25 (H-7 of $\text{R}_1$ and $\text{R}_2$ , m), 7.01 and 7.02 (H-2 of $\text{R}_1$ and $\text{R}_2$ , ss), 6.92 (H-5(6) of $\text{R}_1$ and $\text{R}_2$ , d)

<sup>a</sup> Chemical shifts were taken on a Varian XL-200 MHz instrument on samples of 1.0 mg of dipeptide/0.5 mL of solvent. Chemical shifts are given in parts per million (ppm) downfield from  $\text{Me}_4\text{Si}$  as internal standard. Letters s, d, dd, t, and m stand for singlet, doublet, doublet of doublet, triplet, and multiplet, respectively. Approximate error is  $\pm 0.05$  ppm. Assignments, when given, are based on published work.<sup>17</sup>

<sup>b</sup> Unresolved signals preclude assignments.

mode-locked argon ion laser (Spectra Physics 171UV). Under normal operating conditions the  $\text{Ar}^+$  laser produces a highly stable train of ca. 120-ps pulses at a repetition frequency of 81.949 MHz and the average mode-locked power was ca. 500 mW. The high repetition frequency of the dye laser output was reduced to 100 MHz by inserting the Bragg cell (Spectra Physics 344 S-454 cavity dumper) in the dye laser cavity, with the Rhodamine 6G as the lasing dye, the average laser power was 25 mW (at 400-KHz repetition frequency), and the pulse duration was 15 ps (measured on Spectra Physics Model 409 autocorrelator). The second harmonic (295 nm, vertically polarized) was generated by means of a temperature tuned ADA crystal. The residual 590-nm radiation was removed by a 7-54 Corning glass cutoff filter. The "Start" signal for the ORTEC 457 TAC was obtained from a portion of the 590-nm pulses via a Texas Instruments TIED 56 photoiodine and an ORTEC 436 discriminator. The emission, viewed at  $90^\circ$ , was passed through an ultraviolet Polacoat polarizer (oM type, 105 UV WRMR) set at  $54.7^\circ$  for lifetime and  $0^\circ$  ( $I_{\parallel}(t)$ ) or  $90^\circ$  ( $I_{\perp}(t)$ ) for anisotropy determinations. Photon counting and data treatment by the Marquardt algorithm have been previously described.<sup>16</sup> Lack of any instrumental artifact was demonstrated by reproducing the published lifetime of among others *N*-acetyltryptophan amide in water  $2.82 \pm 0.04$  ns using a single exponential decay function.

Thin layer chromatography was performed on precoated silica gel 60F<sub>254</sub> plates manufactured by E. Merck, Darmstadt, Germany, using chloroform-ethyl acetate (1:1) ( $\text{S}_1$ ), chloroform-methanol-glacial acetic acid (90:10:0:3) ( $\text{S}_2$ ), or 1-butanol-water-glacial acetic acid (7:2:1) ( $\text{S}_3$ ). Absolute viscosities were determined by density measurements.

## Results and Discussion

Table I gives the chemical shifts of **1**, **2**, **3**, and cyclic L-Trp-L-Trp in  $\text{Me}_2\text{SO}-d_6$ . Chemical shifts of the enantiomers **1**<sub>DD</sub> and **1**<sub>LL</sub> or **1**<sub>DL</sub> and **1**<sub>LD</sub> are seen to be identical. Conversely there are pronounced differences in the chemical shifts, particularly in the aromatic region, between diastereomers **1**<sub>DD</sub> and **1**<sub>DL</sub> or **1**<sub>LL</sub> and **1**<sub>LD</sub>. Similar results (not shown) were obtained in  $\text{MeOH}-d_4$  and in  $\text{CH}_3\text{CN}-d_3$ . The chemical shift of the H-2 proton of the indole ring is known to be sensitive to the environment.<sup>17</sup> The observed upfield shifts of this proton in **3** (7.12 ppm) with respect to that in **2** (7.20 ppm) has been interpreted to imply an interaction between the indole ring and dipeptide backbone in L-Ala-L-Trp-OH.<sup>9</sup> Steric effect makes it difficult to have a charge-transfer interaction between the carbonyl group of the peptide bond and the indole ring in **2** but not in **3**. It is, therefore, not unreasonable to assume that the upfield shift of H-2 proton in **3** is due to the charge-transfer interaction between indole ring and the carbonyl

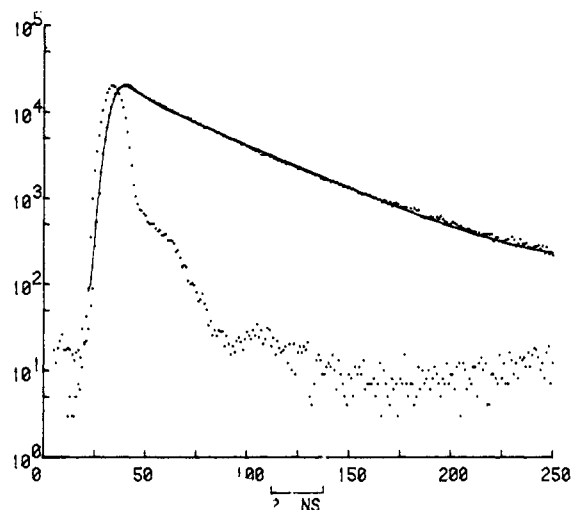


Figure 2. Fluorescence decay plot of **1**<sub>LL</sub> in 78.5% glycerol-methanol (w/v). The fast decay dots show the instrument response function, while the slower decay dots represent the fluorescence decay due to **1**<sub>LL</sub>. The solid line drawn was calculated to give  $\tau_1 = 2.96$  ns (53% at  $t = 0$ ) and  $\tau_2 = 0.93$  ns with  $\chi^2 = 1.4$ .

group of the peptide bond. The H-2 proton signal in indole rings of **1**<sub>LL</sub> (or **1**<sub>DD</sub>) is a singlet at 7.19 ppm while the H-2's in **1**<sub>DL</sub> (or **1**<sub>LD</sub>) are two doublets at 7.09 and 7.11 ppm. There are two H-2's in **1**; with our present spectra, it is very difficult to assign which of the H-2's correspond to 7.09 and 7.11 ppm. The only reasonable explanation is that two H-2 in **1**<sub>LL</sub> (or **1**<sub>DD</sub>) have very little interaction with each other or with the peptide backbone (no shift).<sup>17</sup> Also they appear to be in the same environment. Conversely, two H-2 in **1**<sub>DL</sub> (or **1**<sub>LD</sub>) are two doublets and are shifted upfield (11 and 9 ppm) which suggests that there is a strong interaction between the indole rings with the backbone and with each other. It also implies that the two indole rings of **1**<sub>DL</sub> (or **1**<sub>LD</sub>) are in different environments.<sup>18</sup> H-2's in cyclic L-Trp-L-Trp behave in the same way as that of **1**<sub>DL</sub> (or **1**<sub>LD</sub>): two singlet at 7.01 and 7.02 ppm. Steady-state polarization,<sup>19</sup> CD,<sup>20,21</sup> and NMR<sup>17</sup> studies have shown that for a diketopiperazine having two aromatic residues with the L configuration (cyclic L-Tyr-L-Tyr

(16) Beddard, G. S.; Fleming, G. R.; Porter, G.; Robbins, R. *Philos. Trans. R. Soc. London, Ser. A* **1980**, *298*, 321.

(17) Cohen, J. S. *Biochim. Biophys. Acta* **1971**, *229*, 603. Skrabal, P.; Rizzo, V.; Baici, A.; Bangerter, F.; Luisi, P. L. *Biopolymers* **1979**, *18*, 995. Baici, A.; Rizzo, V.; Skrabal, P.; Luisi, P. L. *J. Am. Chem. Soc.* **1979**, *101*, 5170. Lande, S. *Biopolymers* **1969**, *7*, 879. Lemieux, R. V.; Barton, M. A. *Can. J. Chem.* **1971**, *49*, 767.

(18) Feeney, J. *Proc. R. Soc. London, Ser. A* **1975**, *345*, 61.

(19) Edelhoch, H.; Bernstein, R. S.; Wilcheck, M. *J. Biol. Chem.* **1968**, *243*, 5985.

(20) Edelhoch, H.; Lippoldt, R. E.; Wilcheck, M. *J. Biol. Chem.* **1968**, *243*, 4799.

(21) Strickland, E. H.; Wilcheck, M.; Horowitz, J.; Billups, C. *J. Biol. Chem.* **1970**, *245*, 4168.

**Table II.** Fluorescence Decay Times ( $\tau_1$ ,  $\tau_2$ ,  $\tau_m$ ) and Anisotropies ( $\tau_R$ ) for Tryptophan Derivatives in Different Solvents (in nanoseconds)<sup>a</sup>

	$\tau_1$	$\tau_2$	$\tau_f$	$\tau_m$	$\tau_R$
In DMSO					
L-Trp-L-Trp-OMe	7.02	1.48	0.79	5.85	
D-Trp-L-Trp-OMe	6.64	2.25	0.71	5.36	
cyclic L-Trp-L-Trp	6.21	1.65	0.64	4.57	
L-Trp-L-Ala-OH	7.89	1.40	0.81	6.66	
L-Ala-L-Trp-OH	8.44	3.26	0.77	7.25	
In MeOH					
L-Trp-L-Trp-OMe	2.80	0.88	0.57	1.97	
D-Trp-L-Trp-OMe	2.70	0.95	0.44	1.72	
In CH <sub>3</sub> CN					
L-Trp-L-Trp-OMe	4.59	1.57	0.66	3.56	
D-Trp-L-Trp-OMe	4.88	1.99	0.72	4.07	
L-Trp-L-Ala-OH	5.44	1.06	0.79	4.52	
L-Ala-L-Trp-OH	4.59	1.77	0.75	3.89	
In Glycerol-MeOH Mixture <sup>b</sup>					
L-Trp-L-Trp-OH 68%	3.59	1.0	0.46	2.19	
93%	4.68	0.89	0.61	3.12	
L-Trp-L-Trp-OMe 61.8%					1.36
68.5%	2.37	0.72	0.47	1.49	
70.8%					1.96
78.5%					2.97
86.5%					5.50
93.5%	3.42	0.73	0.61	2.37	
D-Trp-L-Trp-OMe 61.8%					1.35
68.5%	2.33	0.75	0.35	1.30	
70.8%					2.19
78.5%					2.60
86.5%					6.61
93.5%	3.10	0.84	0.55	2.68	
N-acetyltryptophan amide 70.6%					0
In 1,4-pentandiol					
L-Trp-L-Trp-OMe					2.89
In 1,5-Pentandiol					
L-Trp-L-Trp-OMe					2.10
In Undecanol					
L-Trp-L-Trp-OMe					1.0

<sup>a</sup> Defined as  $I(t) = A(e^{-t/\tau_1} + (1-f)e^{-t/\tau_2}) + B$ , where  $A$  is the amplitude and  $B$  the background. Convolution of this equation with shifting between the laser profile and fluorescence was performed as described elsewhere.<sup>16</sup>  $\tau_m = f\tau_1 + (1-f)\tau_2$ . Errors  $\pm 3\%$  on each measurement. <sup>b</sup> Several measurements were taken between these mixture % lifetime fall linearly between the values given.

and cyclic L-Trp-L-Trp), the most stable conformers are the one having both aromatic side chains sharing the space over the diketopiperazine ring. Our NMR results can be interpreted thus: in the ground state, **1<sub>LL</sub>** (or **1<sub>DD</sub>**) has an open form while the **1<sub>DL</sub>** (or **1<sub>LD</sub>**) achieves a folded form with the two indole rings interacting with the backbone and with each other.

Fluorescence decay and anisotropy measurements provide evidence for conformational differences in **1<sub>DL</sub>** and **1<sub>LL</sub>** in the excited states. Fluorescence decay times of the dipeptides in Me<sub>2</sub>SO, MeCN, MeOH, and Glycerol-MeOH mixtures are (at least) biexponential (Figure 2 and Table II). The differences in decay times between **1<sub>DL</sub>** and **1<sub>LL</sub>** reflect different degrees of quenching of the chromophores due to different conformations. Quenching of **1** by CCl<sub>4</sub> in MeOH produced Stern-Volmer constants of  $34 \pm 1.1 \text{ M}^{-1}$  for **1<sub>LL</sub>** and  $27 \pm 0.6 \text{ M}^{-1}$  for **1<sub>DL</sub>**. The difference, however, disappears when mean decay times were used (Table II) to calculate the quenching rate constants ( $k = \tau_m K_{sv}$  where  $\tau_m$  = mean decay time;  $K_{sv}$  = Stern-Volmer quenching constant)  $k_{LL} = 1.7 \times 10^{10} \text{ M}^{-1} \text{ s}^{-1}$  and  $k_{DL} = 1.60 \times 10^{10} \text{ M}^{-1} \text{ s}^{-1}$ . As the rate of quenching is close to being diffusion controlled and also as the chromophores are readily accessible to the quencher, a lack of stereoselectivity is to be expected. This may not be the case in cyclic Trp-Trp which has a Stern-Volmer quenching constant of  $8.8 \pm 0.5 \text{ M}^{-1}$  and a similar mean decay time as **1<sub>DL</sub>** and **1<sub>LL</sub>**.

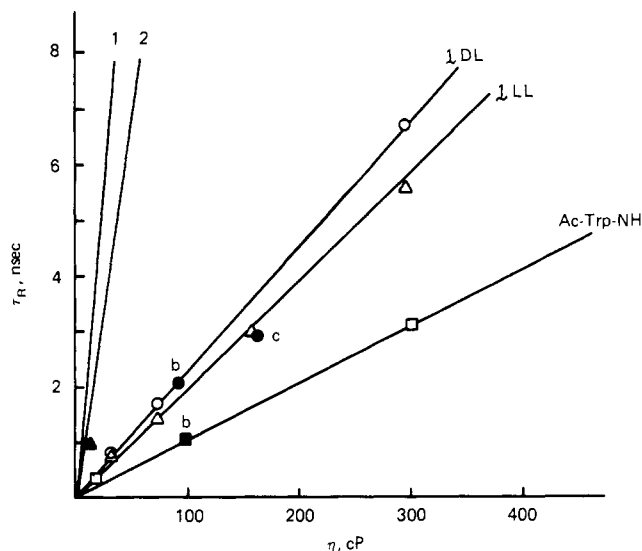


**Figure 3.** Plots of rotational correlation times ( $\tau_R$ ) vs. solvent viscosities ( $\eta$ ) for **1<sub>DL</sub>** (○), **1<sub>LL</sub>** (Δ), and *N*-acetyltryptophan amide<sup>12</sup> according to eq 2 in glycerol-methanol mixtures unless indicated otherwise by letters next to the filled symbols: a = 1,5-pentandiol, b = 1,5-pentandiol, and c = 1,4-pentandiol. Lines 1 and 2 were calculated from eq 2 based on the "stick condition" and using respectively 420- and 300-Å<sup>3</sup> volumes. A line coinciding with the data points for **1<sub>DL</sub>** was calculated from eq 2 using the "slip condition" and 420 Å<sup>3</sup>.

The quenching rate of cyclic Trp-Trp by CCl<sub>4</sub> is, therefore, much slower compared to **1<sub>DL</sub>** and **1<sub>LL</sub>**. This may be due to the shielding of the indole groups from the CCl<sub>4</sub>.

The anisotropy in the fluorescence was used to measure the rate of rotational relaxation of **1<sub>DL</sub>**, **1<sub>LD</sub>** in glycerol-MeOH mixtures. The anisotropy is defined<sup>22,23</sup> by

$$f(t) = (I_{\parallel}(t) - I_{\perp}(t)) / (I_{\parallel}(t) + 2I_{\perp}(t)) \quad (1)$$

with  $I_{\parallel}$  and  $I_{\perp}$  the (time-dependent) fluorescence intensities observed through polarizers parallel and perpendicularly oriented to the vertically polarized excitation. The intensities were suitably normalized to one another. For a rotating sphere in a continuous medium the second order rotational correlation time is given by<sup>24</sup>

$$\tau_R = 8\pi\eta R^3 k / 6\kappa_B T \quad (2)$$

where  $\eta$  is the bulk viscosity of the medium,  $R$  the radius of the rotating molecule,  $\kappa_B$  the Boltzmann constant, and  $T$  the absolute temperature. The constant  $k$  depends upon the boundary condition,  $k = 1$  for stick. Under slip boundary conditions  $k < 1$ . Hu and Zwanzig<sup>25</sup> and Youngren and Acrivos<sup>26</sup> have analyzed the reorientation of spheroidal and ellipsoidal molecules respectively. In the general case  $r(t)$  is the sum of 5 exponential decay terms.<sup>24</sup> When the dipole is along the symmetry axis, thus reducing and treating the molecule as an ellipsoid,<sup>22</sup> the anisotropy is related to the rotational correlation time  $\tau_R$  by  $r(t) = r_0 e^{-t/\tau_R}$ . Experimentally, only exponentially decaying anisotropies were observed. From plots of  $\tau_R$  vs.  $\eta$  (solvent viscosity), Figure 3, viscosity dependence of 21.2 and 17.1 ps/cP are calculated for **1<sub>DL</sub>** and **1<sub>LL</sub>**, respectively. With the assumption for the moment that eq 2 is applicable and  $k = 1$  substituting appropriate viscosities, the corresponding volume for **1<sub>DL</sub>** and **1<sub>LL</sub>** are 87.2 and 70.4 Å<sup>3</sup>, respectively, from anisotropy measurements and 81.3 and 60.3 Å<sup>3</sup>, respectively, from Perrin plots obtained from steady-state

(22) Cherry, R. J.; Nigg, E.; Beddard, G. S. *Proc. Natl. Acad. Sci. U.S.A.* **1980**, *77*, 5899.

(23) Reed, W.; Politi, M.; Fendler, J. H. *J. Am. Chem. Soc.* **1981**, *103*, 4591.

(24) Lessing, H. E.; von Jena, A.; Reichert, M. *Chem. Phys. Lett.* **1975**, *36*, 517. Fleming, G. R.; Morris, J. M.; Robinson, G. W. *Chem. Phys.* **1976**, *17*, 91.

(25) Hu, C.; Zwanzig, R. *J. Chem. Phys.* **1974**, *60*, 4354.

(26) Youngren, G. K.; Acrivos, A. *J. Chem. Phys.* **1975**, *63*, 3846.

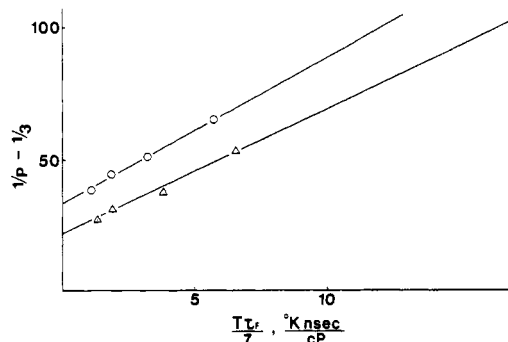


**Figure 4.** Plots of  $(1/P - 1/3)/(1/P_0 - 1/3)$  against  $V$  for  $1_{DL}$  ( $\odot$ ) and  $1_{LL}$  ( $\Delta$ ) according to Perrin's equation  $(1/P - 1/3)/(1/P_0 - 1/3) = 1 + RT\tau_F/\eta V$ , where  $P$  = polarization at a given viscosity,  $P_0$  = polarization at infinite viscosity,  $R$  = gas constant,  $\tau_F$  = mean fluorescence lifetime,  $\eta$  = viscosity of the medium, and  $V$  = effective volume.

polarization measurements (Figure 4).

Inspection of space-filling models of **1** indicates molecular volumes of either  $420 \pm 40 \text{ \AA}^3$ , assuming that the indole rings are facing each other (an oblate shape with an axial ratio of 0.5), or  $300 \pm 40 \text{ \AA}^3$  when the shape is prolate with an axial ratio of 3 and when the indoles are far from one another. These values are at least three times larger than those obtained experimentally and are similar to rotation volumes obtained for molecules such as Rhodamine 6G ( $414 \text{ \AA}^3$ ) or methylred ( $242 \text{ \AA}^3$ ).<sup>27</sup> The volumes measured for **1** ( $\sim 80 \text{ \AA}^3$ ) are similar to those calculated for small molecules such as benzene ( $80 \text{ \AA}^3$ ) or toluene ( $97 \text{ \AA}^3$ ).<sup>28</sup>

It is well-known that a viscous fluid moving relative to a macroscopic surface obeys a stick boundary condition. Examples are provided by many dye molecules as determined by matching of the experimental and calculated (from molecular shape) rotational correlation times.<sup>24</sup> For many dyes in glycerol and in dihydric alcohols faster rotational reorientational times have been observed than those predicted based on the stick conditions.<sup>29</sup> A similar behavior to that in glycerol-MeOH was observed by 1,4-pentanediol and 1,5-pentanediol, the values for the reorientation times in these solvents falling close to values in the glycerol-MeOH at the same macroscopic viscosity. In 1-undecanol, however, the reorientation time (1.0 ns) is much larger (by ca. 3 times) than anticipated from the previous results. The 1.0-ns reorientation time is fairly close but still below the line predicted for "stick" behavior. Similarly, reorientation times for *N*-acetyltryptophan amide were measured to fall in line with those previously reported for glycerol-H<sub>2</sub>O<sup>12</sup> and ethylene glycol<sup>27</sup> but on a line below that for stick behavior.

Rayleigh light scattering experiments have demonstrated that different reorientational behavior is to be expected between monohydric and dihydric alcohols.<sup>30</sup> If there are regions of short-range order in the liquid which are continuously breaking and reforming, this effect can be thought of as fluctuations in the local free volume. Molecular reorientation can occur when sufficient free volume becomes available. If this persists for a short time, then the molecule can only reorient over some small angle and then stops. This leads to a diffusion model where the reorientation is in small random steps. If the fluctuations persist for a longer time, reorientation over large angles can occur and is limited by the time scale of the fluctuations then a jump model applies. Undecanol reorients by the diffusion model and glycerol by the jump model—presumably because a number of bonds must be broken simultaneously for reorientation to occur. The diols are intermediate in their behaviors. The results of **1** in these different solvents may be rationalized in terms of the different solvent behaviors. In undecanol, behavior close to stick is observed where "Brownian diffusion" of the solvent occurs. In glycerol-

MeOH the longer fluctuations in the solvent allow **1** to reorient in the interstices in the solvent and rotational behavior faster than stick limit is observed.

Evidence is also accumulating for the validity of the slip boundary condition for small molecules such as benzene and benzoic acids whose molecular rotation is only impeded by the necessity to displace the solvent molecules. The possible applicability of the slip condition for **1** is by the very much smaller measured than calculated rotation volume. With use of the formula to correct for the molecular shape being nonspherical, the diffusion coefficients,  $D_{\parallel}$  and  $D_{\perp}$  can be calculated from tabulated values for the ratio of friction coefficients for stick to slip.<sup>25,28</sup> This correction when used with a  $420\text{-}\text{\AA}^3$  molecular volume (folded shape) of **1** gives a viscosity dependence of 26 ps/cP in good agreement with that obtained experimentally (21.2 ps/cP). The viscosity dependence for the prolate shape (open shape) of **1** is 31 ps/cP is slightly more than experimental value. Similarity of the calculated and observed gradients of  $\tau_R$  vs.  $\eta$  may be misleading, however, in a molecule containing two similar chromophores for the motion of the two indole groups with respect to one another and the possibility of reversible energy transfer between the two chromophores must be considered as both can lead to fluorescence depolarization. We shall discuss the anisotropy and decay properties of **1** under the four conditions obtained by combining rapid or fixed motion of the Trp groups during the excited-state decay time with fast and slow reversible energy transfer (RET) between the two indoles also during the excited-state decay time.

1. In the first case we consider the Trp-Trp motion to be fixed but RET is to be fast. Under these conditions the  $r_0$  value (the anisotropy at time zero) but not the decay of  $r(t)$  should be affected. Furthermore, the contribution to  $r_0$  due to energy transfer should only fall to  $\sim 0.5$  of the value for tryptophan alone at the excitation wavelength used. If Trp-Trp dipoles are parallel or antiparallel, then RET does not affect  $r_0$  or  $r(t)$  but, if the dipoles are nearly perpendicular, then not only will RET be slowed but also it will cause fluorescence depolarization since the "effective emission dipole" direction will be midway between the two dipoles. This RET process will not explain the low  $P_0$  (or  $r_0$ ) value obtained from the Perrin plots (Figure 1G) or the rapid  $\tau_R$  observed. Also since the molecular dimensions in this case do not change, RET rates should be independent of solvent viscosity.

2. When Trp-Trp motion is fixed and RET is slow or absent, the  $r_0$  (or  $P_0$ ) value should be an average value of the orientations of the two emission dipoles. When the dipoles are parallel (in the  $L_a$  transition in which the dipole is approximately along an axis of the indole nitrogen atom and indole  $C_4$ ), the Trp-Trp compounds behave as if only one Trp is present. If the Trp dipoles are approximately perpendicular, then  $r_0 \rightarrow 0$  ( $P_0 \rightarrow 0$ ) and no or very little anisotropy should be observed (even though the rate of anisotropy decay is unchanged; i.e., molecular rotation is unaffected). An angle of  $\sim 70^\circ$  (or  $\sim 110^\circ$ ) between the two dipoles would reduce the  $P_0$  value to  $\sim 0.10$  of that from tryptophan alone as is observed approximately; i.e.,  $P_0$  for  $1_{DL} = 0.03$ , for  $1_{LL} = 0.05$ , and for tryptophan = 2.5. The  $\tau_R$  values assuming stick boundary condition, however, should be approximately 3 times larger than those measured.

3. If the Trp-Trp groups move during the excited-state lifetime but again is RET  $\rightarrow 0$  then depolarization should occur provided, the motion is perpendicular to the emission dipole axis. With the indole groups connected at carbon  $C_3$ , motion from  $C_\alpha$  to the indole  $C_3$  (see formula) should depolarize the fluorescence since the dipole is approximately perpendicular to this axis. The  $r_0$  (or  $P_0$ ) value in this situation will be the dynamic average of the two emission dipole directions and, as is the previous case, can take value between 0 and its maximum value.<sup>31</sup> An average angle of  $\sim 70^\circ$  or  $\sim 110^\circ$  between the dipoles would give the observed  $P_0$  values. The rotational lifetime  $\tau_R$  could, however, be much shorter than

(27) von Jena, H.; Lessing, H. *Chem. Phys.* **1979**, *40*, 245.

(28) Bauer, D. R.; Brauman, J. I.; Pecora, R. *J. Am. Chem. Soc.* **1974**, *96*, 6840.

(29) Rice, S. A.; Kenny-Wallace, G. *Chem. Phys.* **1980**, *47*, 161.

(30) Pinnow, D.; Candau, S.; Litovitz, T. *J. Chem. Phys.* **1968**, *40*, 347.

(31) Dale, R.; Eisinger, J. In "Biochemical Fluorescence Concepts"; Chen, R., Edelhoch, H., Eds.; Marcel Dekker: New York, 1975; Vol. 1, pp 115-284, and references cited therein.

anticipated as the internal motion would appear as a rotation of the whole molecule.

4. In the fourth and final case, we consider rapid Trp-Trp motion as well as fast RET then the situation is complex but related to the first case since reversible energy transfer reorients the emission dipoles. Some information of the properties of the Trp-Trp can be obtained from the fluorescence decay measurements. The decays for Trp, Trp-Ala, and Ala-Trp are generally nonexponential and depend on the pH of solution.<sup>9,16</sup> In Trp-Trp the decays are also nonexponential. Proton-transfer and charge-transfer quenching have been shown to describe the behavior of Trp, Ala-Trp, and Trp-Ala at neutral pH.<sup>9,16</sup> Lifetimes due to different rotamers have also been proposed.<sup>32</sup> Charge transfer is favored for Trp-Trp in Me<sub>2</sub>SO or MeCN since the amino group is not protonated. The two decay times could be due to diffusional motion of the chromophore into the correct geometry for quenching; alternatively the two lifetimes could be due to different quenching rates of the two indole rings by the carbonyl group.

### Conclusions

Both NMR and fluorescence anisotropy experiments clearly illustrate the differences in shape of the **1**<sub>LL</sub> and **1**<sub>DL</sub> diastereomers. We have postulated that the **1**<sub>DL</sub> has a folded structure and **1**<sub>LL</sub> a more open geometry with respect to the indole chromophores. The reorientational relaxation of **1** in glycerol-MeOH mixtures

and in dihydric alcohol are far faster than anticipated by using stick limit boundary conditions; in fact the slip limit fits the data points fairly well. This "slip-like" type of behavior has been previously observed in glycerol and may be a consequence of the glycerol reorientation occurring by large steps rather than by Brownian diffusion as a result of long-lived volume fluctuation in this liquid. **1** rotates with more freedom as a result of these fluctuations than in undecanol which orients by a small-jump diffusional process.<sup>30</sup> In glycerol-MeOH it is also possible that the two indoles in the molecule rotate during the excited state lifetime and contribute to the overall molecular rotation. This intramolecular motion would be aided by the freedom to rotational motion allowed in the glycerol-MeOH mixtures. The small *P*<sub>0</sub> values obtained from Perrin plots can be explained if the two indole chromophores emission dipoles are ~70° or ~110° to one another. Energy transfer between the two indole would be small compared to the excited-state lifetime when the chromophores have these geometries.

**Acknowledgment** is made to the donors of the Petroleum Research Fund, administered by the American Chemical Society. We are grateful to Dr. J. Feeney (NIMR, Mill Hill, London) for assistance in the interpretation of the NMR spectra.

**Registry No.** **1**<sub>LL</sub>, 81387-96-4; **1**<sub>DL</sub>, 81387-97-5; **1**<sub>DD</sub>, 81387-98-6; **1**<sub>LD</sub>, 81387-99-7; **2**, 24046-71-7; **3**, 16305-75-2; Z-L-Trp-OH, 7432-21-5; Z-D-Trp-OH, 2279-15-4; H-L-Trp-OMe-HCl, 26988-71-6; H-D-Trp-OMe-HCl, 41222-70-2; Z-Trp-Trp-OMe, 17689-58-6; Z-D-Trp-Trp-OMe, 81444-73-7; Z-D-Trp-D-Trp-OMe, 81444-74-8; Z-Trp-D-Trp-OMe, 81444-75-9; cyclo(Trp-Trp), 20829-55-4.

(32) Szabo, A. G.; Rayner, D. M. *J. Am. Chem. Soc.* **1980**, *102*, 554.

## Sign Determination of Electron-Spin Distributions in Iminoxy Radical Analogues

Graham R. Underwood\* and Karam El Bayoumy

Contribution from the Department of Chemistry, New York University, Washington Square, New York, New York 10003. Received May 1, 1980

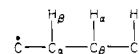
**Abstract:** Nickel-induced <sup>1</sup>H NMR contact shifts have been determined for β, γ, δ, and ε protons in a variety of oximes in which the molecular geometries are partially constrained by the oximino group. It is shown that these represent appropriate models for iminoxy radicals, with electron spin induced primarily in the nitrogen lone-pair orbital. Since this method directly provides the sign of the electron-spin density, it permits inference of the signs in the iminoxy radicals. It is pointed out that spin distributions in these radical analogues parallel those similarly determined in aliphatic and aromatic amines, thus indicating spin delocalization independence of the nature (σ or π) of the intervening bonds in the molecule.

The study of long-range ESR hyperfine splitting constants (hfsc's) has provided considerable insight into electron and electron-spin delocalization through σ frameworks and hence into the quantum mechanical integrals controlling these and related phenomena.<sup>1</sup> These data can be rationalized simplistically but usefully within the valence bond formalism, thus providing mnemonics for the prediction of the effect on spin densities of such variables as structure, conformation, substitution, etc. In developing a fuller picture of the mechanisms of spin delocalization, major advances have been made by studying the effect of molecular geometry on the ESR hfsc's particularly in rigid bicyclic radicals, by quantum mechanical analysis of the data, and by experimental determination of the sign of the spin density.<sup>1</sup>

Since the modes of spin delocalization are determined to a large extent by the orientation of the bonds making up the delocalization paths, it is necessary to be able to describe these paths unam-

biguously in terms of the relevant dihedral angles in that molecular fragment. The convention used for defining these angles, θ<sub>β</sub><sup>C</sup>, θ<sub>γ</sub><sup>H</sup>, etc., is illustrated in Figure 1 by using the nonplanar propyl fragment. Mechanisms of spin delocalization to α and β nuclei<sup>2</sup> have been well established<sup>3</sup> and, while considerable progress has been made with delocalization to nuclei more distant from the radical site, the difficulty in obtaining sufficient experiment data for certain regions of conformational space has been a limiting factor. In particular, data in the regions (180°, 0°) and (0°, 180°)

(2) The nomenclature adopted here is the usual ESR convention, viz.



(3) (a) H. M. McConnell, *J. Chem. Phys.* **24**, 764 (1956); (b) R. Bersohn, *ibid.*, **24**, 1066 (1956); (c) H. S. Jarrett, *ibid.*, **25**, 1289 (1956); (d) H. M. McConnell and D. B. Chesnut, *ibid.*, **28**, 107 (1958); (e) B. Venkataraman and G. K. Fraenkel, *J. Am. Chem. Soc.*, **77**, 2707 (1955); (f) R. Bersohn, *J. Chem. Phys.*, **24**, 1066 (1956); (g) J. P. Colpa and E. de Boer, *Mol. Phys.*, **7**, 333 (1964).

(1) For a recent thorough review of this subject see F. W. King, *Chem. Rev.*, **76**, 157 (1976).